Induction Machine Modelling Using Permeance Network Method for Dynamic Simulation of Air-Gap Eccentricity

A. Mahyob, M. Y Ould Elmoctar, P. Reghem, G. Barakat
GREAH, Groupe de Recherche en Electrotechnique et Automatique du Havre
University of Le Havre, 25 rue Philippe Lebon, BP 540
76058 Le Havre, France
Tel.: +33 / (0) – 232744336
Fax: +33 / (0) – 232744348.
(*e-mail:* amin.mahyob@univ-lehavre.fr , georges.barakat@univ-lehavre.fr)
URL: http://www.univ-lehavre.fr/greah

Keywords

« Electrical machines », « Modelling », « Simulation, », « Induction machine », « diagnostic »

Abstract

Electrical machines diagnosis needs a modelling approach reliable and as close to the reality as possible. It is shown that by proper modelling of the induction machine it is possible to detect the effect of the different faults on the machine current and vibrations. This paper proposes a model based on Permeance Network Method (PNM) for the simulation of faulty induction machines. The PNM allows the authors to take into account the local magnetic saturation and remains moderately time consuming compared to the finite element method. The developed permeance network of the machine is coupled to the stator phase electrical equations on one side and, on the other side, to the mechanical motion equation in order to simulate variable speed operations. The air-gap eccentricity is then taken into account in the modelling of the air-gap permeance. The effect of the eccentricity on the current and vibration signatures is discussed. Theoretical analysis for the effect of the machine eccentricity is presented.

I. Introduction

In recent years, the use of three phase induction machine in critical applications occupies a significant field. It is appreciated for its robustness and its low cost This-increasing of use requiring high safety level. The ever-increasing requirements for reliability and cost reduction have squared the research on early fault detection, on condition monitoring and non-invasive diagnosis of the operating conditions of induction motors, [1]-[2. Condition monitoring can significantly reduce the maintenance cost and the risk of unexpected failures by allowing the early detection of potentially catastrophic faults. The key for the success is to have accurate means of condition assessment and fault diagnosis.

Eccentricity related faults constitute an important portion of the faulty induction machine. Machine eccentricity means unequal air-gap that exists between the rotor and stator. There are two types of air-gap eccentricity, the static air-gap eccentricity and dynamic air gap eccentricity. En reality static and dynamic eccentricities tend to coexist. In electrical machines an inherent level of static eccentricity exists due to manufacturing and assembling method [3].This minimum are-gap eccentricity level is acceptable and it is kept by good designs, but the eccentricity level increase after the installation of the machine and running for several years. High eccentricity levels can result in rotor to stator rub and consequential damage to the stator core and high voltage winding. This results in motor failure and expensive repair. Higher than the normal levels of air-gap eccentricity can produce high vibrations in the bearing and subsequent bearing failure [4]-[5]-[6]-[7].

Most of the recent researches dealing with faulty induction machines have developed diagnosis techniques based on the motor current signature analysis (MCSA) to sense motor faults [1]-[2]-[8],-[9].The success of MCSA methods depends on their accuracy of measurements and on their ability to discriminate between various faults generating the same range of harmonics in the stator current spectrum. Therefore, the availability of simulation model in the case of faulty machine becomes attractive.

Then, the objective of this paper is to develop an accurate and reasonably complicated model which is capable of predicting the performances of induction machines under different electrical and mecanical faults. The proposed model is based on a permeance network approach and the differential equation system governing the induction machine behavior. The proposed method allows us to easily take into the account some nonlinearities such as the saturation of the magnetic materials and the rotor movement. With simulation time very weak compared to the finite element method.

II. PNM Modelling of the Induction Machine

II. 1. Magnetic Equivalent Circuit Modelling

A. Development of Permeance Network

An electrical machine can be represented as a set of flux tubes (Fig. 1), characterized by their magnetic permeances which depend on the magnetic permeability and the geometry of the flux tube considered [10]-[11]-[12]]-[18].
On a two dimensional assumption, electrical machine geometry can be divided into elementary areas.
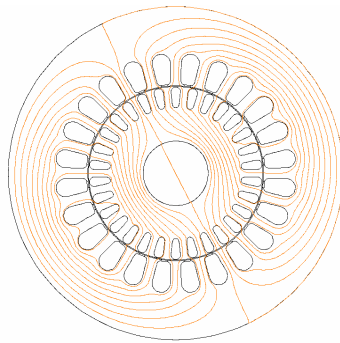
Fig.1. Flux tubes of the studied machine

For an induction machine we define an elementary magnetic circuit constituted by a slot and its associated tooth and yoke sections .this elementary circuit appears in both rotor and stator. The permeances of an elementary circuit are expressed as function of the machine geometry and fluxes flowing in each one of its elements.

To take into account the magnetic circuit saturation, the B-H curve is modelled thanks to Marrocco's formula [13] which is used to calculate the relative reluctivity of each flux tube. This reluctivity is given by:

$$\frac{1}{\mu_r} = v_r = \varepsilon + (c - \varepsilon)\frac{B^{2\alpha}}{B^{2\alpha} + \tau} \tag{1}$$

where ε, c, α and τ are constants depending on the magnetisation curve.

Rotation movement is taken in consideration through the air-gap element .effectively, when the rotor moves, only air-gap permeances vary. So, we define a permeance evolution law connecting a stator tooth to rotor tooth as presented in (2) [10]. This permeance depends on the relative position of these teeth θ_{ij}.

$$P_{i,j} = \begin{cases} P_{max} & 0 \le \theta \le \gamma_t' \ et\ 2\pi - \gamma_t' \le \theta \le 2\pi \\ P_{max}\left(1+cos\pi\ \dfrac{\theta_{ij}-\gamma_t'}{\gamma_t-\gamma_t'}\right)\Big/2 & \gamma_t' \le \theta_{ij} \le \gamma_t \\ P_{max}\left(1+cos\pi\ \dfrac{\theta_{ij}-2\pi+\gamma_t'}{\gamma_t-\gamma_t'}\right)\Big/2 & 2\pi - \gamma_t \le \theta_{ij} \le 2\pi - \gamma_t' \\ 0 & else \end{cases} \tag{2}$$

The different parameters in the air-gap permeance expression are expressed in terms of the stator and rotor slot dimensions. Figure 2 illustrates the general form airgap permeance (in μH) between stator and rotor teeth that have different widths at the air gap level
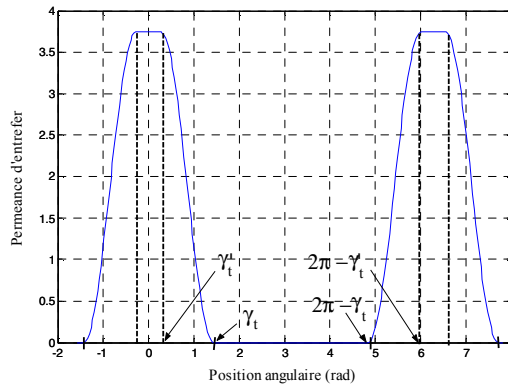
Fig.2 Air-gap permeance between stator and rotor teeth

The armature reaction is modeled as m.m.f. in series with the tooth permeance. The relation between this m.m.f. and the phase currents can be given by the following matrix form:

$$\left[F_t\right] = \left[M_i\right]\left[I\right] \tag{3}$$

where $\left[F_t\right]$ is the vector of tooth m.m.f., $\left[I\right]$ is the vector of the phase currents and $\left[M_i\right]$ is the matrix that relates the teeth electromagnetic forces to the phase current.

Applying the approach described above, one can deduce the magnetic equivalent circuit shown in Fig.3

B. Setting of Magnetic Equations

It is seen that the magnetic equivalent circuit consists of branches, permeances, and supplies of m.m.f. of coils and bars connected by nodes. Thus one can set magnetic equations with the same way as in electric circuits. In our case node and branch equations are written considering stator phase and rotor loop currents as the entry of the system. These equations are given by the following general form:

$$\begin{bmatrix} [\Re] & [N^t] \\ [N] & [P] \end{bmatrix} \cdot \begin{bmatrix} [\Phi_t] \\ [U] \end{bmatrix} = \begin{bmatrix} [M_i] \\ [0] \end{bmatrix} \cdot [I] \tag{4}$$

where $[\Re]$ is the diagonal reluctance matrix, $[P]$ is the permeance matrix, $[\Phi_t]$ is the vector of stator and rotor tooth fluxes, $[U]$ is the vector of stator and rotor node scalar magnetic potential, $[M_i]$ is the matrix that relates the tooth electromagnetic forces to the phase current and $[I]$ is the vector of stator and rotor currents.
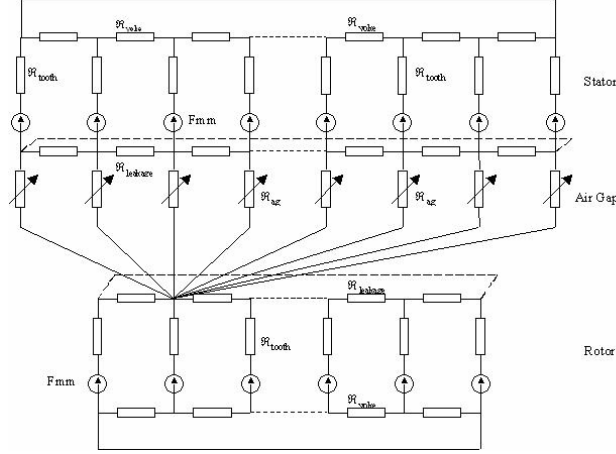
Fig. 3 Permeance Network of studied machine

II.2. Electric Circuit Modelling

Consider initially a general m-phase induction machine with q rotor bars. The proposed model is derived from a well-known method [14] consisting in replacing the q bars squirrel cage by an equivalent circuit containing $q+1$ magnetically coupled meshes as shown in figure 4.

The equations describing the general induction machine with m stator phases and q rotor bars can be written in vector-matrix form and in a compact manner as follows:

$$[V] = [R][I] + [L_\sigma] \frac{d}{dt}[I] + \frac{d}{dt}[\psi] \tag{5}$$

where $[R] = \begin{bmatrix} [R_{SS}] & [0] \\ [0] & [R_{RR}] \end{bmatrix}$; $[L_\sigma] = \begin{bmatrix} [L_{\sigma S}] & [0] \\ [0] & [L_{\sigma R}] \end{bmatrix}$ and $[\psi] = \begin{bmatrix} [\psi_S] \\ [\psi_R] \end{bmatrix} = \begin{bmatrix} [M_{\phi S}] & [0] \\ 0 & [M_{\phi R}] \end{bmatrix} \cdot \begin{bmatrix} [\Phi_S] \\ [\Phi_R] \end{bmatrix}$

$[V]$ Is the vector of stator and rotor voltages, $[I]$ is the vector of stator and rotor currents. $[R]$ is the resistance matrix, $[L_\sigma]$ is winding head and end ring leakage inductance matrix, $M_{\phi s}$ is the matrix that relates the phase linkage fluxes to the tooth fluxes , $M_{\phi r}$ is the matrix that relates the mesh linkage fluxes to the tooth fluxes and $[\psi]$ is the linkage flux vector.

II.3: Motion Equation

To the set of magnetic and electric equations one must add the mechanical equation of the shaft. The torque equation is established by deriving the magnetic co-energy with respect to the rotor angular position; thus the electromagnetic torque obtained is given by/

$$T_{em} = \frac{1}{2} \sum_{i=1}^{Ns} \sum_{j=1}^{Nr} \frac{dP_{i,j}}{d\theta} U_{i,j}^2 \tag{6}$$

And the mechanical equation is given by:

$$T_{em} = T_{res} + J \frac{d\Omega}{dt} + f_{frot} \Omega \tag{7}$$

where Ω is the rotor angular speed and θ_m is the rotor position. $U_{i,j}$ is the scalar magnetic potential between the stator tooth 'i' and the rotor tooth 'j'.

The attractive force (radial force) between the stator and rotor is calculated by deriving the magnetic co-energy with respect to the effective air-gap length δ [10].This force is given by:

$$F_r = \frac{1}{2} \sum_{i=1}^{Ns} \sum_{j=1}^{Nr} \frac{dP_{i,j}}{d\delta} U_{i,j}^2 \qquad (8)$$
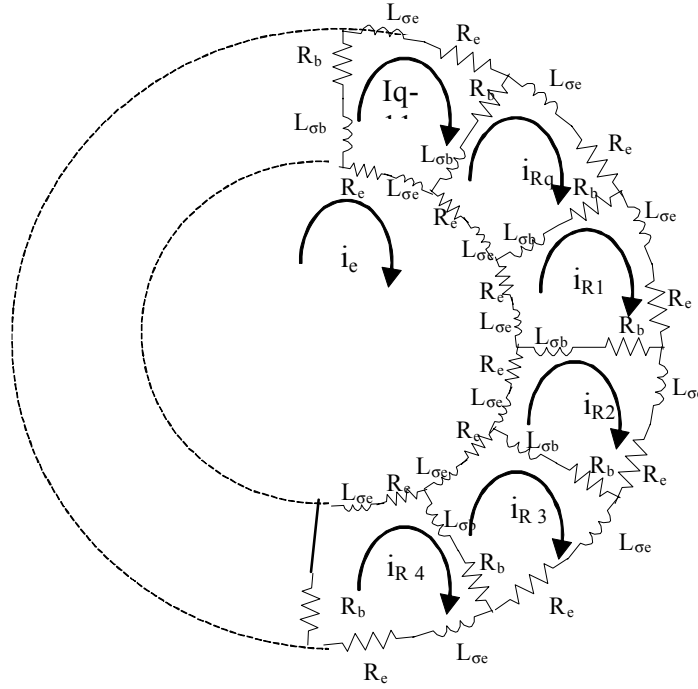
Fig.4. Equivalent circuit of the rotor cage showing the meshes

III. Modelling of Air-Gap Eccentricity

When static eccentricity occurs in a cylindrical machine, the rotor rotates around its axis; [9]-[16]-[17], in this case the effective air-gap becomes irregular and then, the effective air-gap length varies sinusoidally with the angular position in the stator frame, thus the maximum air gap permeance is different from one stator tooth to an other depending their position with respect to the reference statoric. The effective air-gap length corresponding to the stator tooth *i* can be approximated by:

$$\delta_i(\theta_s) = \delta_0(1 - \varepsilon \cos \theta_{si}) \qquad (9)$$

where ε is the per unit eccentricity of the rotor (the distance between the rotor and stator axis) and θ_{si} Indicates the position of the stator tooth *i* with respect to the position corresponding to the minimum air-gap effective length and In this case, the minimum air-gap length does not revolve with the rotor position. However, in the case of dynamic eccentricity the rotor rotates around the stator axis and in this case the minimum air-gap length revolves with rotor position; the effective air-gap length corresponding to the stator tooth *i* can be approximated by:

$$\delta_i(\theta, \theta_s) = \delta_0(1 - \varepsilon \cos(\theta_{si} - \theta)) \qquad (10)$$

One should note that in this case the permeance seen by all stator teeth will be the same.
In the case of mixed eccentricity where the rotor rotates around an axis usually lies between its axis and the stator axis and parallel to them, the effective air-gap length corresponding to the stator tooth *i* can be approximated by:[3]-[18]

$$\delta_i(\theta, \theta_s) \cong \delta_0(1 - \varepsilon_{mix} \cos(\theta_{si} - \theta_{mix}(\theta))) \qquad (11)$$

with :

$$\varepsilon_{mix}(\theta) = \sqrt{\varepsilon_s^2 + \varepsilon_d^2 + 2\varepsilon_s\varepsilon_d \cos(\theta)}$$
$$\theta_{mix}(\theta) = arctan(\frac{\varepsilon_d \sin(\theta)}{\varepsilon_s + \varepsilon_d \cos(\theta)})$$

(12)

where ε_s is the per unit static eccentricity of the rotor and ε_d is the per unit dynamic eccentricity (the distance between the stator axis and the axis of rotation).To avoid the rotor –stator rub, $\varepsilon_s + \varepsilon_d < 1$

To introduce of the eccentricity faults into the model previously developed the permeance function given by (2) will be scaled by the eccentricity factor given by:

$$C_i = \frac{\delta_0}{\delta(\theta_i)}$$

(13)

where δ_0 is the air-gap length in the normal case and $\delta(\theta_i)$ is the air-gap length in the presence of the eccentricity and it is given by (9) , (10) and(11) depending on the type of eccentricity [10]-[12].

IV: Analysis of Force, Torque, and Current Signals

Air-gap eccentricity in induction machines is usually detected by analyzing the stator line-current spectra. Harmonics in the current spectra of a machine are a result of voltage harmonics induced in the winding by air gap flux density harmonics. As a result, the frequencies of induced current harmonics can be determined by calculating the frequencies of air gap flux density harmonics when viewed from the stationary reference frame. In the absence of detailed designs, basic designs parameters such as numbers of slots can be used to predict the air gap flux density harmonic frequencies. In the analytical model air-gap flux density is given by [15]:

$$B_{gap}(\theta,\theta_s) = [F_s(\theta,\theta_s) + F_r(\theta,\theta_s)]P(\theta,\theta_s)$$

(14)

In (14), $Fs(\theta,\theta_s)$ denotes the stator winding MMF, $Fr(\theta, \theta_s)$ denotes the MMF due to the rotor cage and $P(\theta, \theta_s)$ denotes air gap permeance.

Using Fourier series to describe *MMF and P(θ, θs),* the equation that describes such frequency components for eccentricity is given by [3] [17]

$$f_h = \left[(kq \pm n_d)\frac{(1-s)}{p} \pm v \right] f$$

(15)

where

q is the number of rotor slots, n_d=0   in the case of static eccentricity, n_d =1, 2, 3 . . .in the case of dynamic eccentricity (n_d is known as eccentricity order), f is the fundamental supply frequency, s is the slip, p is the number of fundamental pole pair and, v is the order of the stator time harmonics that are present in the power supply driving the motor (v =1,3,5…etc) and k=1,2,3.

The principal slot harmonic are also given by the above equation with n_d =0, v= 1,k=1.

In the presence of mixed eccentricity, some low frequency components appear in the stator current spectrum independent of Nr and P combination these components are given by:

$$f_{lh} = \left| f \pm kf_r \right|$$

(16)

where f_r is the mechanical speed of the machine in Hertz.

Eccentricity also can be detected by analyzing the bearing vibrations due to Unbalanced magnetic Pull (UMP) which is associated with eccentricity [17]. Analytically the vibration can be analyzed by the analysis of the radial force or the electromagnetic torque harmonics. The equation that describes such

frequency components is the same as (15) with v=0, 2, 4…etc. in addition to the harmonics characterize the magnetic unbalance of the rotor of order $2ksf$, The static eccentricity causes the significant increase in the harmonic of double supply frequency in the torque and radial force. This harmonic led to vibrate the carcass of the machines. The dynamic eccentricity produce other non double supply frequencies such as $f, 2f+f_r, f_{r,}$, and $2(f+f_r)$ [17]. The measurement of these vibrations can be used to detect the eccentricity and distinguish between the different types of eccentricity.

V. Simulation Results and Discussion

The proposed model has been used in a simulation study of a 4 kW, 2-poles, 24 stator slots, 30-bars squirrel cage. The detailed parameters of the machine are given in the appendix.

Figure 5 shows the FFT of stator phase current for healthy and eccentric machine at 5.6% slip. It is shown that all the types of the eccentricity the same range of current harmonics closed to those given by (15). It is seen that it may not be possible to detect the eccentricities and distinguish between their types by comparing only the magnitudes of these harmonics, but the comparison between the
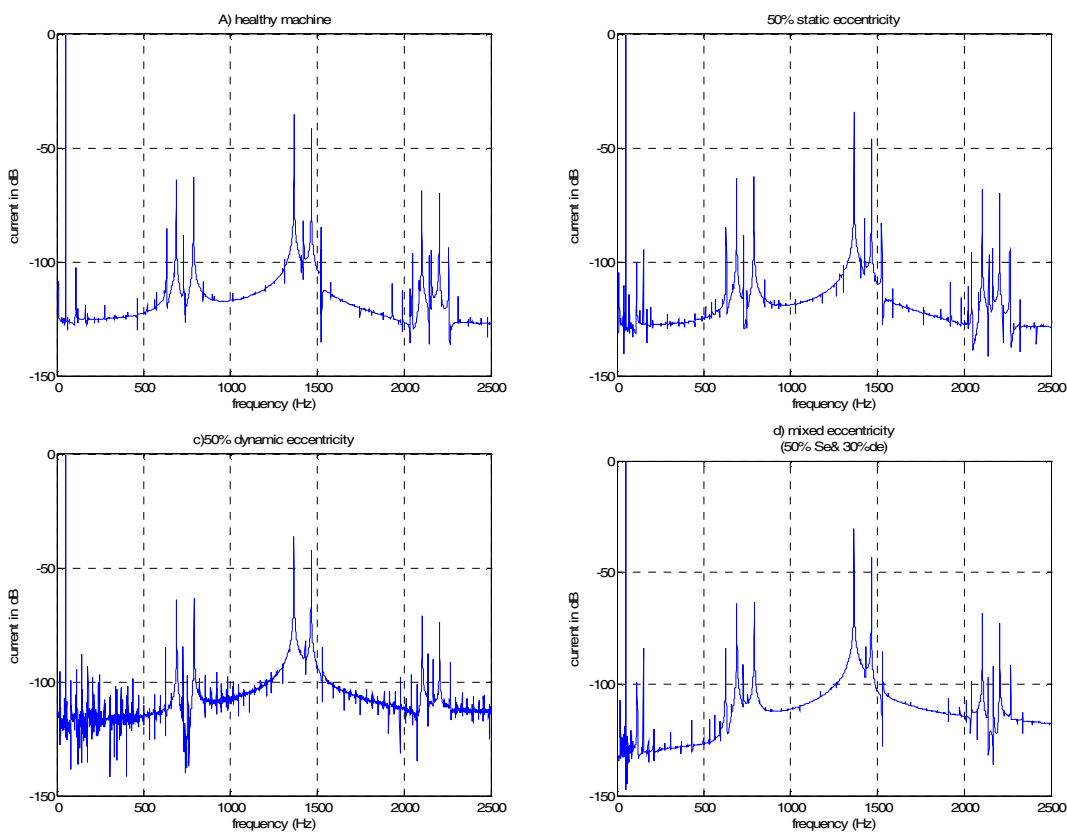
Fig (5) Normalized stator current spectrum for healthy machine and different cases of eccentricity

sidebands at the fundamental and the slots harmonics corresponding for each type helps to detect the eccentricities and to differentiate between them as it is shown on the fig.5.

Figures 6 shows the FFT of the radial force for healthy and eccentric machine at 5.6% slip. The analysis of the radial force shows that static and mixed eccentricities give a rise in twice supply frequency harmonic, but the dynamic eccentricity has little effect on this frequency. On the other hand, in the presence of dynamic eccentricity new harmonics appear neighbour of this frequency. It is also shown that the power spectral density neighbour the fundamental and slots harmonics is different form one type of eccentricity to other.

VI. Conclusion

In this paper, a reluctance network based model to simulate faulty induction machine has been presented. The model was tested by comparing the results obtained by the model of healthy machine with machine data and the results obtained by the method of finite elements. The Results were closed to each other. This model takes into account the saturation magnetic and doubly slotted air-gap as well as the rotor movement. This model allows to study more precisely the effects of eccentricity on the machine performances as well as to give a robust model of simulation for the model-based diagnosis method. The proposed model was used to simulate the dynamic behaviour of a conventional induction machine with airgap eccentricity. Other works are in progress to combine eccentricity faults with the other stator and rotor faults such as inter-turns, broken rotor bars and rotor end rings faults. Fault signature characterized by the developed model is used for the induction machine monitoring.
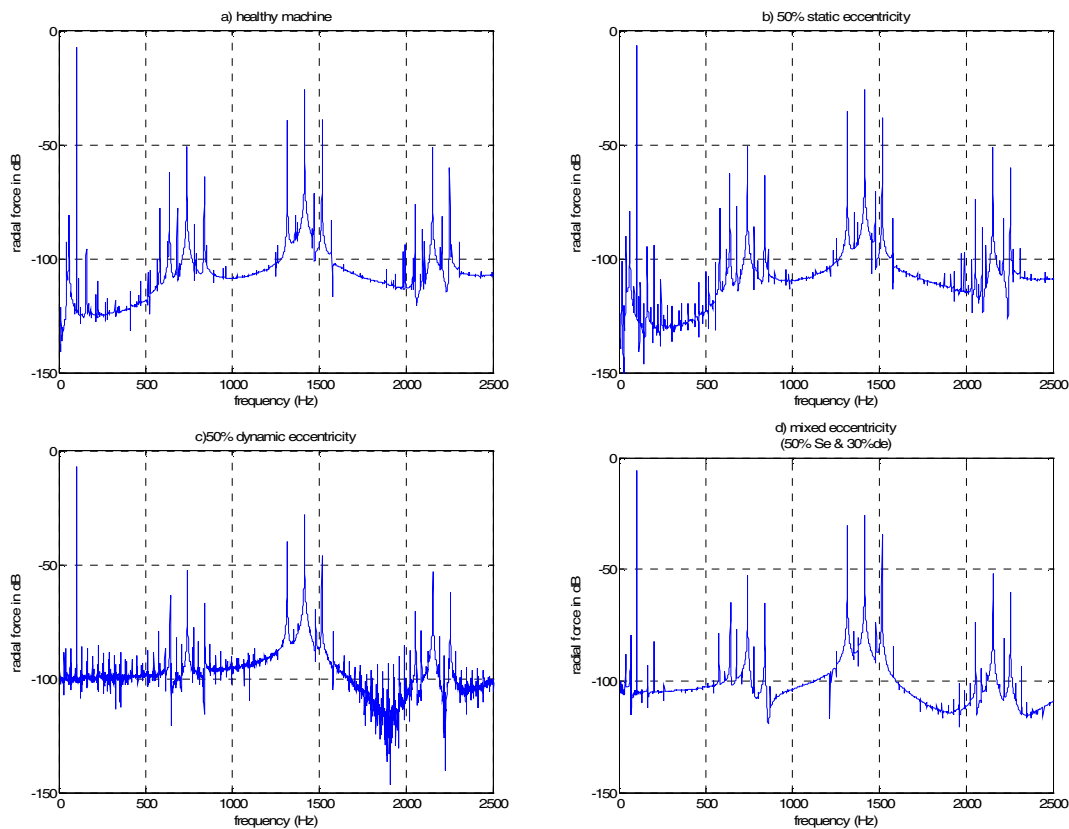
Fig (5) Normalized radial force spectrum for healthy machine and different cases of eccentricity

Appendix

Studied motor parameters:
4 kW, 230/400 V, 14.2/8.2 A, 2840 rpm, 2 poles, 24 stator slots, 30 rotor bars

D_{so} = 145 mm	stator outer diameter
D_{si} = 75.4 mm	stator inner diameter
L_s = 125 mm	stack length
D_{sh} = 31.5 mm	shaft diameter
e = 0.35 mm	effective airgap
R_r = 37.35 mm	rotor radius
β = 1.4	bar skew coefficient
s_s = 2.6 mm	stator slot opening width
b_s = 5.78 mm	stator slot base length
d_s = 0.6 mm	stator slot isthmus width

$s_r = 1.1$ mm	rotor slot opening width
$b_r = 4.0$ mm	rotor slot base length
$d_r = 0.9$ mm	rotor slot isthmus width
$N_s = 124$	# of stator phase turns in series
$R_s = 1.595$ Ω	stator phase resistance
$L_s = 0.004$ H	stator phase leakage inductance
$R_b = 3.04\text{E-04}$ Ω	rotor bar resistance
$L_b = 5.16\text{E-07}$ H	rotor bar leakage inductance
$R_e = 8.75\text{E-07}$ Ω	rotor end ring segment resistance
$L_e = 1.59\text{E-09}$ H	rotor end ring segment leakage inductance
$J = 0.045$ kg.m2	drive inertia
$f_v = 0.0038$ kg.m^2.s^{-1}	friction coefficient

References

[1] J.P. Tavner and J. Penman, Condition Monitoring of Electrical Machines. *Research Studies Press Ltd.* Letchworth, Herfordshire, U.K.,1987.

[2] W.T. Thomson, "A Review of on-line Condition Monitoring Techniques for Three-Phase Squirrel-Cage Induction Motors -Past Present and Future," *IEEE International Symposium on Diagnostics for Electrical Machines, Power Electronics and Drives*, Gijón, September 1999, pp. 3-18.

[3] S. Nandi, R. Bharadwaj and H. Toliyat, "Performance analysis of a three phase induction motor under mixed eccentricity condition*," IEEE Trans.Energy Convers.*, vol. 17, no. 3, pp. 392–399, Sep. 2002.

[4] W. Thomson, D. Rankin, and D. Dorrell, "On-line current monitoring to diagnose airgap eccentricity in large three-phase induction motors—Industrial case histories verify the predictions," *IEEE Trans. Energy Convers.*,vol. 14, no. 4, pp. 1372–1378, Dec. 1999.

[5] W. Thomson and A. Barbour, "On-line current monitoring and application of a finite element method to predict the level of static airgap eccentricity in three-phase induction motors," *IEEE Trans. Energy Convers.*, vol. 13,no. 4, pp. 347–357, Dec. 1998.

[6] S. I. Nau, R.Beck, N Sadowski, ''The influence of the eccentricity on the magnetic noise on the three phase induction motot: an experimental approach'', *ICEM 2002*. 25 - 28.8.2002. Bruges, Belgium.

[7] A. Tenhunen T. P. Holopainen and A. Arkkio, "Spatial linearity of unbalanced magnetic pull in induction motors during eccentric rotor motions", *ICEM 2002*,CD-ROM 25 - 28.8.2002. Bruges, Belgium.

[8] M.E.H. Benbouzid, "A review of induction motors signature analysis as a medium for faults detection," *IEEE Trans. Ind. Electron.*, vol. 47, no. 5, pp. 984-993, Oct, 2000

[9] G. Barakat, G. Houdouin, B. Dakyo, AND E. Destobbeleer, **"**An improved method for dynamic simulation of air-gap eccentricity in induction machines,**"** in Proc. *IEEE SDEMPED*'01*,* Grado, Italy, Sept. 2001, pp. 133-138.

[10] V.Ostovic, *Dynamics of Saturated Electric Machines*, spring -Verlag, New York, 1989.

[11] C. Delforge, B. Lemaire-smail, "Induction machine modelling using finite elements and permeance network methods", *IEEE Trans. Magn.*, Vol.,31,No. 3, pp. 2092-2095, May 1995.

[12] Nicola Jerance, Gillles Rostaing, J.P. Rognon and Albert Forggia, "Induction machine modelling by reluctance network for fault diagnostic", in *Proc. Electrimacs 2002*, CD-ROM, Montreal, Canada, 18-21 Aug. 2002.

[13] A. Marrocco, "Analyse numérique de problèmes d'électrotechnique," *Ann.Sc.math*, Québec, vol. 1, pp. 271-296, 1977.

[14] M. Poloujadoff, "The theory of three phase induction squirrel cage machine," *Electric Machines and Power Systems*, vol. 13, pp 245-264, 1987.

[15] Andrew M. Knight, , and Sergio P. Bertani, "Mechanical Fault Detection in a Medium-Sized Induction Motor Using Stator Current Monitoring'', *IEEE Trans. Energy Convers*, Vol. 20, No. 4,pp.753-760, December 2005.

[16] H. A. Toliyat, M. S. Arefeen *and* A. G. Parlos, "A method for dynamic simulation of air-gap eccentricity in induction machines*," IEEE Trans. Ind. Applicat.*, vol. 32, no. 4, pp. 910-917, Jul./Aug. 1996.

[17] D. Dorrel, W. Thomson, and S. Roach, "Analysis of airgap flux, current and vibration signals as a function of the combination of static and dynamic airgap eccentricity of 3-phase induction motors," *IEEE Trans. Ind. Appl.*,vol. 33, no. 1, pp. 24–34, Jan./Feb. 1997.

[18] M; derrhi, C. Delforge, P. Brochet, ,'fault simulation of induction machine using a coupled permeance network model'', *International workshop SDEMPED*, pp401-406, Dijon, Spain, 163 sept. 1999.